

promoting access to White Rose research papers



Universities of Leeds, Sheffield and York
<http://eprints.whiterose.ac.uk/>

This is a copy of the final published version of a paper published via gold open access in **Mechanical Systems and Signal Processing**.

This open access article is distributed under the terms of the Creative Commons Attribution Licence (<http://creativecommons.org/licenses/by/3.0>), which permits unrestricted use, distribution, and reproduction in any medium, provided the original work is properly cited.

White Rose Research Online URL for this paper:
<http://eprints.whiterose.ac.uk/83948>

Published paper

Green, P.L., Cross, E.J. and Worden, K. (2014) Bayesian system identification of dynamical systems using highly informative training data. *Mechanical Systems and Signal Processing*, 56. 109 - 122. Doi: 10.1016/j.ymssp.2014.10.003



ELSEVIER

Contents lists available at ScienceDirect

Mechanical Systems and Signal Processing

journal homepage: www.elsevier.com/locate/ymssp

Bayesian system identification of dynamical systems using highly informative training data



P.L. Green*, E.J. Cross, K. Worden

Department of Mechanical Engineering, University of Sheffield, Mappin Street, Sheffield S1 3JD, United Kingdom

ARTICLE INFO

Article history:

Received 5 July 2013

Received in revised form

20 May 2014

Accepted 9 October 2014

Available online 4 November 2014

Keywords:

Nonlinear system identification

Bayesian inference

Markov chain Monte Carlo

Shannon entropy

Tamar bridge

ABSTRACT

This paper is concerned with the Bayesian system identification of structural dynamical systems using experimentally obtained training data. It is motivated by situations where, from a large quantity of training data, one must select a subset to infer probabilistic models. To that end, using concepts from information theory, expressions are derived which allow one to approximate the effect that a set of training data will have on parameter uncertainty as well as the plausibility of candidate model structures. The usefulness of this concept is then demonstrated through the system identification of several dynamical systems using both physics-based and emulator models. The result is a rigorous scientific framework which can be used to select 'highly informative' subsets from large quantities of training data.

© 2014 The Authors. Published by Elsevier Ltd. This is an open access article under the CC BY license (<http://creativecommons.org/licenses/by/3.0/>).

1. Introduction

To be practically useful, any system identification method needs to be able to quantify and propagate the inevitable uncertainties which arise as a result of noise-contaminated measurements, as well as the fact that one's chosen model structure will never be able to perfectly replicate the physics of the system of interest. Consequently, system identification is best approached using probability logic such that, rather than searching for the 'perfect model', one is able to assess the relative plausibility of a set of models as well as the parameters within those models [1]. As a result of seminal papers in the machine learning [2] and structural dynamics [3] communities, it is now widely accepted that both levels of inference (parameter estimation and model selection) can be achieved using a Bayesian approach.

With regard to parameter estimation, the plausibility of a model parameter vector $\theta = \{\theta_1, \dots, \theta_{N_\theta}\}$ given a model structure \mathcal{M} and training data \mathcal{D} can be expressed using Bayes' Theorem:

$$P(\theta|\mathcal{D}, \mathcal{M}) = \frac{P(\mathcal{D}|\theta, \mathcal{M})P(\theta|\mathcal{M})}{P(\mathcal{D}|\mathcal{M})}. \quad (1)$$

One's belief in the plausibility of θ before the training data were known is represented by the prior distribution $P(\theta|\mathcal{M})$, while one's belief in the plausibility of θ after the training data are known is represented in the posterior distribution $P(\theta|\mathcal{D}, \mathcal{M})$. $P(\mathcal{D}|\theta, \mathcal{M})$ is termed the likelihood and represents the plausibility that the training data \mathcal{D} was witnessed given

* Corresponding author.

E-mail addresses: p.l.green@sheffield.ac.uk (P.L. Green), e.j.cross@sheffield.ac.uk (E.J. Cross), k.worden@sheffield.ac.uk (K. Worden).

model structure \mathcal{M} and parameter vector θ . The evidence $P(\mathcal{D}|\mathcal{M})$ is essentially a normalising constant given by

$$P(\mathcal{D}|\mathcal{M}) = \int \dots \int P(\mathcal{D}|\theta, \mathcal{M})P(\theta|\mathcal{M})d\theta_1 \dots d\theta_{N_d} \quad (2)$$

thus ensuring that the posterior probability distribution integrates to unity. When dealing with nonlinear systems, the evidence integral is often intractable and, as a result of the curse of dimensionality, cannot practically be evaluated numerically when the number of unknown parameters is greater than 3.

To surmount this issue one can choose to generate samples from the posterior distribution using Markov chain Monte Carlo (MCMC) methods, which can be implemented without having to evaluate Eq. (2). While many MCMC methods have been developed (see Refs. [4–6] for a comprehensive discussion), by far the most popular is the Metropolis–Hastings (MH) algorithm. This involves the evolution of an ergodic Markov chain through the parameter space such that it is able to converge to, and then generate samples from, the posterior distribution. Ensuring that the chain has converged to the globally optimum region of the parameter space (rather than a ‘local trap’) is a nontrivial problem which has led to the development of the well-known Simulated Annealing algorithm [7] (and its many variants [8–10]) and, more recently, the Adaptive Metropolis–Hastings [11], Transitional Markov chain Monte Carlo [12] and Asymptotically Independent Markov Sampling [13] algorithms.

Once converged, MCMC can then be used to generate samples from the posterior. These samples can be used to analyse parameter correlations, to propagate one’s uncertainty in the parameter estimates and to conduct a sensitivity analysis of the model structure of interest (see [14,15] for example). While undoubtedly useful, MCMC tends to be expensive, as many model runs are usually required before one can build up a reasonable ‘picture’ of the posterior distribution. This is compounded by the fact that, by the nature of MCMC, the samples have not been generated independently and are in fact correlated with each another. Consequently, to avoid making biased estimates, it is often the case that many of the samples generated by MCMC need to be ‘thrown away’ such that the correlation between the remaining samples is reduced (this process is typically referred to as *thinning*). To alleviate this issue one may choose an alternative to the MH algorithm such as Hybrid Monte Carlo (HMC) [16] which tends to produce samples which are less strongly correlated than the MH algorithm (HMC is discussed in the context of structural dynamics in [17]). However, as HMC utilises estimates of the gradient of the posterior distribution – which incurs additional computational cost – the author’s have found that the ability of HMC to outperform the MH algorithm is very dependent on the problem at hand.

To reduce the computational expense of Monte Carlo analysis one may choose to utilise emulators (also known as meta-models or surrogate models) which are inferred directly from the training data rather than from the underlying physics of the system (see [18] for example). The relatively simple structures of emulators often make them considerably easier to analyse, and computationally cheap when compared to physics-based models.

The work in this paper specifically addresses the situation where, to perform Bayesian system identification as part of some collaborative work, one is presented with a very large quantity of data from which to infer probabilistic models. In such a scenario – particularly if one is aiming to utilise physics-based models – it is usually desirable to select a small subset of the training data to reduce the computational cost of running MCMC.¹ In such a scenario one would ideally select a subset of data which is both short and *highly informative* with regard to one’s parameter estimates. Consequently, the first aim of this paper is to provide a framework which allows one to view the information content – specifically with regard to one’s parameter estimates – of large sets of training data *before* the application of MCMC. This allows one to select subsets of data which are both small, and from which one can learn a great deal about the parameters of a candidate model.

The second aim of this paper is with regard to the second level of inference: model selection. Whether using physics-based models or emulators, any system identification procedure will involve choosing a model \mathcal{M} from a set of candidate model structures (as implied by Eq. (1)). This task is complicated by the fact that model performance cannot be judged simply by how well a model is able to replicate a set of training data as this will lead to overfitted models based on redundant parameter sets. This issue can be addressed by using model selection criteria such as the AIC [20] or the BIC [21], which reward model fidelity while also penalising model complexity. Alternatively, one can phrase the model selection problem using Bayes’ Theorem:

$$P(\mathcal{M}_i|\mathcal{D}) = \frac{P(\mathcal{D}|\mathcal{M}_i)P(\mathcal{M}_i)}{P(\mathcal{D})} \quad (3)$$

where \mathcal{M}_i is a model from a set of candidate model structures $\mathbf{M} = \{\mathcal{M}_1, \dots, \mathcal{M}_{N_M}\}$. Assuming that there is no prior bias over any of the models in \mathbf{M} , one can then rate the relative plausibility of two competing model structures (models \mathcal{M}_i and \mathcal{M}_j for example) by computing a Bayes Factor:

$$\beta_{ij} = \frac{P(\mathcal{M}_i|\mathcal{D})}{P(\mathcal{M}_j|\mathcal{D})} \quad (4)$$

The Bayes Factor is a model selection criterion which, it can be shown, penalises overfitting without the introduction of *ad hoc* penalty terms (see [1,2,6,22] for more details). Recent work [23] has also shown that such an approach can also be used

¹ Clearly the computational savings achieved through this approach is dependent on the size of the chosen subset, relative to the full set of training data. In situations where the full set of training data is relatively small, the computational savings that could be made through the methods presented in this paper may be small relative to what can be achieved through the parallel implementation of MCMC algorithms (see [19] for example).

to aid in the selection of the prediction-error model used in the likelihood, although this is not investigated in the present paper.

With the second level of inference in mind then, building on the aforementioned idea of ‘highly informative’ training data, the second major aim of the present work, is to identify which sets of training data will be the most informative with regard to model selection. This develops the idea that an informative set of training data will aid the model selection procedure, by demonstrating that one particular model is much more plausible than the other competing structures.

The paper is organised as follows. Section 2 addresses parameter estimation specifically. Expressions allowing one to approximate the effect of a set of training data on the posterior covariance matrix are derived in Section 2.1, before being linked with concepts from information theory as well as previous work from the machine learning community [24] in Sections 2.2 and 2.3. These concepts are then extended to the case of model selection in Section 3. The various benefits of using highly informative training data with regard to parameter estimation and model selection are demonstrated using a series of examples in Sections 4 and 5, where the system identification of a synthesised nonlinear system using a physics-based model and of the Tamar bridge using an emulator are investigated.

2. Parameter estimation

2.1. Taylor series expansion

The case where there are N_D parameters to be identified (such that $\boldsymbol{\theta} \in \mathbb{R}^{N_D}$) is considered here. The parameters are to be inferred using training data \mathcal{D} which consists of a vector of inputs and corresponding outputs of the system of interest. It is assumed that each measured data point is corrupted by Gaussian white noise with variance σ^2 , such that the likelihood is given by

$$P(\mathcal{D}|\boldsymbol{\theta}, \mathcal{M}) = \prod_{n=1}^N (2\pi\sigma^2)^{-1/2} \exp\left(-\frac{1}{2\sigma^2}(z_n - \hat{z}_n(\boldsymbol{\theta}))^2\right) \quad (5)$$

where z is the measured response of the real system and \hat{z} is the response of the model.

It is well known that, by approximating the log-likelihood ($L(\boldsymbol{\theta})$) using a second-order Taylor series expansion (see [6] for more details) and assuming an uninformative prior, the posterior can be approximated according to

$$P^*(\boldsymbol{\theta}|\mathcal{D}, \mathcal{M}) = \frac{P(\mathcal{D}|\hat{\boldsymbol{\theta}}, \mathcal{M})}{P^*(\mathcal{D}|\mathcal{M})} \exp\left(-\frac{1}{2}[\boldsymbol{\theta} - \hat{\boldsymbol{\theta}}]\mathbf{A}[\boldsymbol{\theta} - \hat{\boldsymbol{\theta}}]^T\right) \quad (6)$$

where $\hat{\boldsymbol{\theta}}$ is the most-probable parameter vector and, throughout this work, asterisks are used to denote quantities which have been approximated in this manner. The matrix \mathbf{A} is the Fisher Information matrix:

$$A_{i,j} = -\left.\frac{\partial^2 L(\boldsymbol{\theta})}{\partial\theta_i \partial\theta_j}\right|_{\boldsymbol{\theta} = \hat{\boldsymbol{\theta}}} \quad (7)$$

whose elements can, depending on the problem at hand, be evaluated analytically or approximated using finite difference methods.

Integrating Eq. (6) with respect to $\boldsymbol{\theta}$ allows one to write the evidence as

$$P^*(\mathcal{D}|\mathcal{M}) = P(\mathcal{D}|\hat{\boldsymbol{\theta}}, \mathcal{M}) \sqrt{\frac{(2\pi)^{N_D}}{|\mathbf{A}|}}. \quad (8)$$

For the sake of clarity, the Gaussian approximation of the posterior will be written as

$$P^*(\boldsymbol{\theta}|\mathcal{D}, \mathcal{M}) = \frac{1}{Z^*} \exp\left(-\frac{1}{2}[\boldsymbol{\theta} - \hat{\boldsymbol{\theta}}]\mathbf{A}[\boldsymbol{\theta} - \hat{\boldsymbol{\theta}}]^T\right) \quad (9)$$

where

$$Z^* = \sqrt{\frac{(2\pi)^{N_D}}{|\mathbf{A}|}}. \quad (10)$$

Although an improper prior distribution has been utilised in this case, it should be noted that the analysis detailed herein will apply to situations where one has employed a uniform prior distribution whose limits are far from the main region of probability mass (it is also relatively easy to extend the arguments presented here to the case where Gaussian priors are used). In fact, such an analysis is not particularly relevant to the concepts presented in this paper because, as it will be shown, the prior distribution has no influence on the informativeness of the training data.

The covariance matrix of $P^*(\boldsymbol{\theta}|\mathcal{D}, \mathcal{M})$ is given by

$$\mathbf{C} = \mathbf{A}^{-1}. \quad (11)$$

If one assumes that the off-diagonal elements of the covariance matrix are negligible then \mathbf{A}^{-1} will be a diagonal matrix with elements:

$$A_{i,i}^{-1} = \left(-\frac{\partial^2 L(\boldsymbol{\theta})}{\partial \theta_i^2} \Big|_{\boldsymbol{\theta} = \hat{\boldsymbol{\theta}}} \right)^{-1} \quad (12)$$

(this is equivalent to assuming that any parameter correlations present in the system are negligible). Consequently, by monitoring the diagonal elements of \mathbf{A} :

$$A_{i,i}^{-1}, \quad i = 1, \dots, N_D \quad (13)$$

as more data points are added to the training data, it is possible to see the effect that these points have on the confidence one has in each individual parameter estimate – a drop in $A_{i,i}^{-1}$ as training data is added indicates that one's confidence in the parameter θ_i has increased. In fact, it was found to be more convenient to monitor

$$\ln(A_{i,i}^{-1}), \quad i = 1, \dots, N_D \quad (14)$$

as training data is added, simply for visualisation purposes. The relative simplicity of this expression is helped largely by the fact that it has been assumed that the covariance matrix is diagonal. In Sections 2.2 and 2.3 of this work it will be shown that this allows one to develop an intuitive interpretation of the Fisher Information matrix as well as an information theoretic interpretation of highly informative training data. However, it is important to recognise that this assumption is not necessary in practice – Eq. (7) can be used to evaluate the 'full' Fisher Information matrix if it is thought to be necessary. Indeed, by doing so, one may be able to monitor the off-diagonal terms of the covariance matrix as training data is added, thus allowing one to assess which parts of the training data will be informative with regard to the parameter correlations. The effect of assuming a diagonal covariance matrix is analysed in more detail through the use of an example in Section 4 of this work.

2.2. Interpretation of the Fisher Information matrix

This section is concerned with the development of a more detailed analysis of the Fisher Information matrix (\mathbf{A}) such that a more complete definition of what is meant by 'informative' training data can be developed.

If one considers the log-likelihood:

$$L(\boldsymbol{\theta}) = -\frac{N}{2} \ln(2\pi\sigma^2) - \frac{1}{2\sigma^2} \sum_{n=1}^N J_n(\boldsymbol{\theta}) \quad (15)$$

(where $J_n = (z_n - \hat{z}_n(\boldsymbol{\theta}))^2$) then, differentiating twice with respect to the elements in the parameter vector and utilising Eq. (7), the Fisher Information Matrix \mathbf{A} becomes

$$\mathbf{A} = \frac{\mathbf{H}}{2\sigma^2} \quad (16)$$

where \mathbf{H} is a Hessian matrix whose elements are defined as

$$H_{i,j} = \sum_{n=1}^N \frac{\partial^2 J_n(\boldsymbol{\theta})}{\partial \theta_i \partial \theta_j} \Big|_{\boldsymbol{\theta} = \hat{\boldsymbol{\theta}}} \quad (17)$$

As a result, the covariance matrix of $P^*(\boldsymbol{\theta}|\mathcal{D}, \mathcal{M})$ is given by

$$\mathbf{C} = 2\sigma^2 \mathbf{H}^{-1}. \quad (18)$$

As before, it is assumed that the off-diagonal terms are zero such that the covariance matrix \mathbf{C} is diagonal with elements given by

$$C_{i,i} = 2\sigma^2 \left(\sum_{n=1}^N \frac{\partial^2 J_n(\boldsymbol{\theta})}{\partial \theta_i^2} \Big|_{\boldsymbol{\theta} = \hat{\boldsymbol{\theta}}} \right)^{-1}. \quad (19)$$

This allows one to define what is meant by the term 'informative' training data. Firstly, Eq. (19) shows that the diagonal elements of the covariance matrix will increase with the measurement noise variance (σ^2). This provides the rather intuitive observation that training data will be more informative if one makes low noise measurements (this point was also made in [24]). Secondly, Eq. (19) shows that one can achieve a large decrease in element $C_{i,i}$ of the covariance matrix through the introduction of a data point for which $\partial^2 J(\boldsymbol{\theta})/\partial \theta_i^2|_{\boldsymbol{\theta} = \hat{\boldsymbol{\theta}}}$ is large. In other words, a point of training data can be considered to be informative (with regard to parameter θ_i) if the ability of the model to replicate that point is very sensitive to changes in θ_i .

2.3. Relation to the Shannon entropy

Intuitively, it seems reasonable to assume that there is a link between the derivation shown in Section 2.1 and information theory. This is because one would say that a data point which has a great effect on one's parameter estimates contains more information than that which has relatively little effect. This concept was investigated as far back as 1992 [24] within the context of machine learning, where the 'informativeness' of training data was analysed using the Shannon entropy as an information measure. While, within the structural dynamics community, it has been shown that the Shannon entropy can be used to optimise sensor placement and/or experimental design (see [25–27] for example), the authors believe that it has not previously been used to analyse the information content – with regard to both levels of Bayesian inference – of large sets of training data.

The main focus of this section is to calculate the Shannon entropy of the posterior such that a relation between the aforementioned work in [24] and that presented in Section 2.1 of the current work can be drawn.

Noting that the Shannon entropy is a measure of uncertainty then, ergo, the aim here is to select a subset of training data which will reduce the Shannon entropy of the posterior as much as possible. It is important at this point to emphasise that this approach is different from that of the Maximum Entropy (MaxEnt) method [28] which, for example, can be used to find the prior distribution which assumes the smallest amount of additional information. In the current paper the term 'highly informative' is not used to describe distributions with large entropy – it is used to refer to data which can greatly reduce the uncertainty in one's parameter estimates and, consequently, the entropy of the posterior distribution.

Using the Gaussian approximation given in Eq. (6), the Shannon entropy of the posterior is given by

$$\begin{aligned} S &= - \int P^*(\boldsymbol{\theta}|\mathcal{D}, \mathcal{M}) \ln(P^*(\boldsymbol{\theta}|\mathcal{D}, \mathcal{M})) d\boldsymbol{\theta} \\ &= \frac{N_D}{2}(\ln(2\pi) + 1) + \frac{1}{2} \ln\left(\frac{1}{|\mathbf{A}|}\right). \end{aligned} \quad (20)$$

If it is assumed that the off-diagonal elements of \mathbf{A} are zero (as in Section 2.1) then the entropy of the posterior becomes

$$S = \frac{N_D}{2}(1 + \ln(2\pi)) + \frac{1}{2} \sum_{i=1}^{N_D} \ln\left(\frac{1}{A_{i,i}}\right). \quad (21)$$

The only term in Eq. (21) which is a function of the training data is $\sum_{i=1}^{N_D} \ln(1/A_{i,i})$ such that by monitoring the quantity

$$S_{i,i} = \ln(A_{i,i}^{-1}), \quad i = 1, \dots, N_D \quad (22)$$

one can see the effect of the training data on the Shannon entropy of the posterior. Consequently then, a link has been drawn between the work demonstrated in [24] and that which is shown in Section 2.1.

3. Model selection

As elaborated in Section 1, one can rate the relative plausibility of two competing model structures using a Bayes Factor. Using the Gaussian approximation of the posterior (Eq. (9)) allows the Bayes Factor between models \mathcal{M}_i and \mathcal{M}_j to be written as

$$\beta_{i,j} = \frac{P(\mathcal{M}_i|\mathcal{D})}{P(\mathcal{M}_j|\mathcal{D})} = \frac{P(\mathcal{D}|\mathcal{M}_i)}{P(\mathcal{D}|\mathcal{M}_j)} \approx \frac{P^*(\mathcal{D}|\mathcal{M}_i)}{P^*(\mathcal{D}|\mathcal{M}_j)} \quad (23)$$

where OF_i and OF_j are used to represent the Occam factors for the model structures \mathcal{M}_i and \mathcal{M}_j respectively. The Occam factor for model i is

$$OF_i = P(\boldsymbol{\theta}|\mathcal{M}_i) \sqrt{\frac{(2\pi)^{N_D^{(i)}}}{|\mathbf{A}^{(i)}|}} \quad (24)$$

where $P(\boldsymbol{\theta}|\mathcal{M}_i)$ is a constant as improper priors are being used, $\mathbf{A}^{(i)}$ is the Fisher Information matrix and $N_D^{(i)}$ is the number of parameters in model structure \mathcal{M}_i . It can be shown that the Occam factor is a term which penalises the model structure of interest for having additional parameters thus helping to prevent overfitting. As it has already been established that one can monitor the diagonal elements of $\mathbf{A}^{(i)}$ and $\mathbf{A}^{(j)}$ as training data is added then it is clear that one will also be able to monitor the Bayes Factor in a similar fashion. This will help to establish which parts of the training data are particularly informative with regard to the model selection procedure as well as helping one to establish that the choice of model is independent of the amount of training data being utilised.

4. Example: system identification of a nonlinear system using physics-based models

The first example considered here is concerned with the system identification of a base-excited SDOF Duffing oscillator (Fig. 1). In order to demonstrate the concept of 'highly informative training data', the analyses detailed in this section were

conducted using simulated training data. The equation of motion of the system is

$$m\ddot{z} + c\dot{z} + kz + k_3z^3 = -m\ddot{y} \tag{25}$$

where m is the mass, c is viscous damping, k is linear stiffness, k_3 is nonlinear stiffness and z represents the relative displacement between the base and the mass:

$$z = x - y. \tag{26}$$

4.1. Parameter estimation

A set of training data was created by simulating the response of the system to a Gaussian white noise input. The resulting relative displacement (z) was then corrupted with Gaussian noise such that the signal to noise ratio of the signal was equal to 20 (Fig. 2). The mass was assumed known, such that the parameter vector to be estimated was $\theta = \{c, k, k_3\}$. The true parameter values and the chosen limits of the uniform prior distribution are shown in Table 1.

For the sake of demonstrating the potential benefits of studying the Shannon entropy of the training data, it is assumed here that the most probable parameter vector $\hat{\theta}$ is known. Firstly, the off-diagonal elements of the Fisher Information matrix were set to zero and the ‘informativeness’ of each parameter was approximated according to Eq. (22). Secondly, the entire Fisher Information matrix was approximated using finite difference methods and, in the same manner, the Shannon entropy of each parameter was evaluated. The resulting entropy estimates are plotted as a function of the number of data points in the training data in Fig. 3.

The first point to note with regard to Fig. 3 is that the values obtained through computation of the full covariance matrix appear to be relatively noisy. This is because inverting the full Fisher Information matrix involves the combination of many more potentially erroneous gradient estimates than if one were to ignore the off-diagonal terms. This is compounded by the fact that estimation of the Hessian matrix requires the approximation of second-order derivatives using finite difference methods. In order to reduce the errors arising in this process, one can utilise the Gauss–Newton method [29] which allows the Hessian to be approximated using only first-order derivatives:

$$H_{ij} \approx 2 \sum_{n=1}^N \frac{\partial r_n}{\partial \theta_i} \frac{\partial r_n}{\partial \theta_j} \tag{27}$$

where $r_n = z_n - \hat{z}_n(\theta)$. Using this method Fig. 4 shows that, relative to the results shown in Fig. 3, the noise present in the estimates made using the full Fisher Information matrix has been greatly reduced.

Fig. 5 shows the estimated Shannon entropy – calculated using the determinant of \mathbf{A} (Eq. (21)). Specifically, the results utilising the full Fisher Information matrix (calculated using the Gauss–Newton method) are compared to those obtained

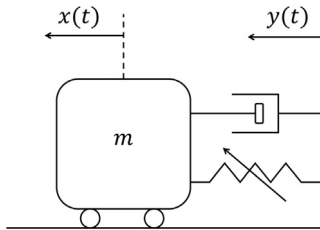


Fig. 1. Base excited Duffing oscillator.

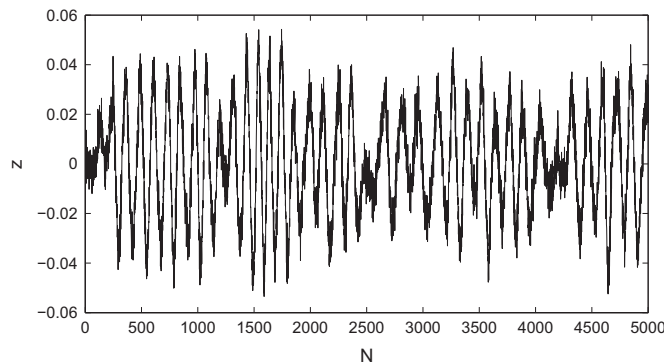


Fig. 2. Training data for parameter estimation of the base excited Duffing oscillator.

Table 1

True parameter values and chosen prior limits for parameter estimation of the base excited Duffing oscillator.

Parameter	True value	Lower prior limit	Upper prior limit	Unit
c	0.1	0	1	N s/m
k	50	0	1×10^3	N/m
k_3	1×10^5	0	1×10^7	N/m ³

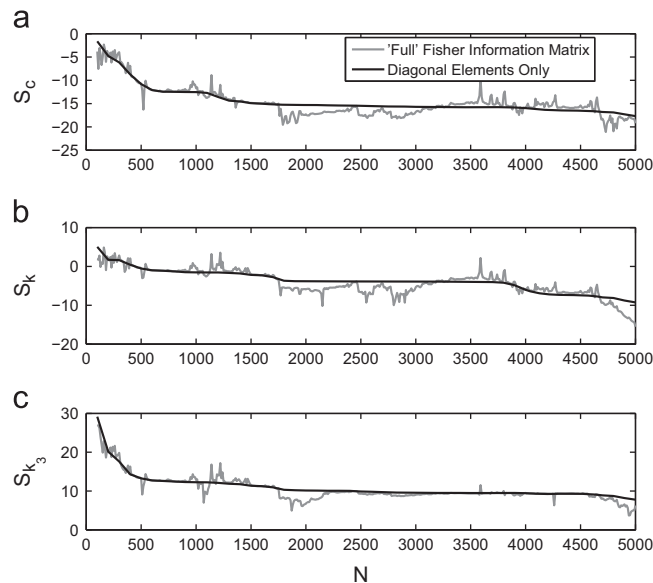


Fig. 3. Parameter estimation of the base-excited Duffing oscillator. The Shannon entropy for parameters (a) c , (b) k and (c) k_3 (evaluated using Eq. (22)). Grey lines represent estimates using the full Fisher Information matrix while black lines represent estimates made using only the diagonal elements of the Fisher Information matrix.

based on assumption of no parameter correlations. While, in this case, both methods produce fairly similar results, it is suggested that the Gauss–Newton method is the more general as its application is not limited to situations where parameter correlations are negligible.

Upon studying the Shannon entropy of each parameter, Figs. 3 and 4 both indicate that if one were to use the first 4500 data points rather than the first 3500 data points of this specific set of training data, then one should realise a more ‘confident’ estimate of the parameter k but still have similar levels of uncertainty with regard to the parameters c and k_3 . To test this hypothesis two sets of MCMC simulations were run – one using the first 3500 data points and one using the first 4500 data points of training data. This was conducted using the Metropolis algorithm. Throughout this paper all MCMC simulations are conducted using the logarithm of the parameters so as to avoid scaling issues. The variances of the proposal densities were tuned such that acceptance ratio of the MH algorithm was roughly 40%.

The resulting Markov chains are shown in Fig. 6. It can be seen that, as predicted, by using the additional 1000 data points the uncertainty in the estimate for k has been reduced greatly while the uncertainty in the other parameters has remained relatively unchanged. Referring back to the training data (Fig. 2), it is interesting to note that it is not obvious exactly why this additional portion of training data has increased our confidence in k so drastically. This is an important result as it shows that plotting the Shannon entropy of the posterior can reveal features of the training data which may not be intuitively obvious.

4.2. Model selection

To investigate the issue of model selection, the response of the base-excited Duffing oscillator to a low amplitude excitation was analysed. This is because, at low amplitudes, the effect of the nonlinear term will be relatively small and so it may be possible to accurately replicate the response of the system over this region of the input space using a linear model. Consequently then, there are two competing model structures: one with k_3 (denoted \mathcal{M}_1) and one without k_3 (denoted \mathcal{M}_2).

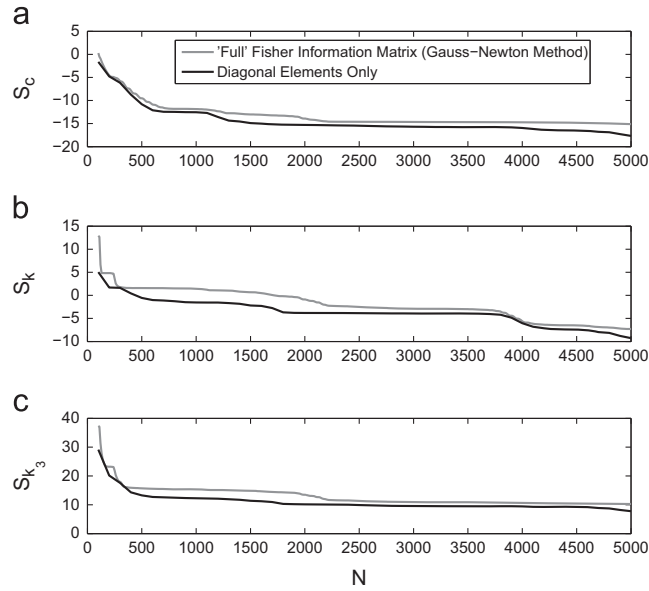


Fig. 4. Parameter estimation of the base-excited Duffing oscillator. The Shannon entropy for parameters (a) c , (b) k and (c) k_3 (evaluated using Eq. (22)). Grey lines represent estimates using the full Fisher Information matrix (Gauss–Newton method) while black lines represent estimates made using only the diagonal elements of the Fisher Information matrix.

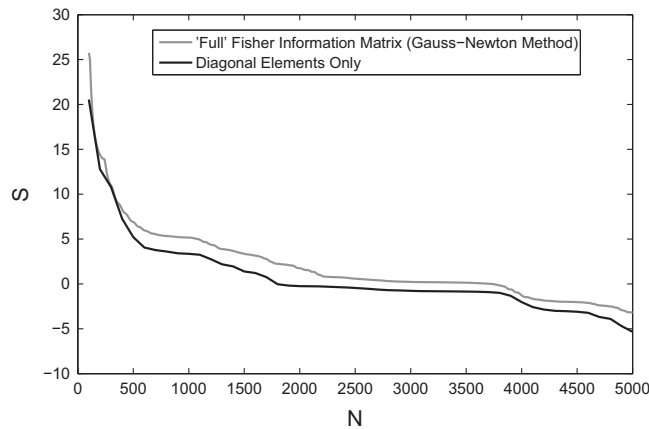


Fig. 5. Parameter estimation of the base-excited Duffing oscillator. The Shannon entropy (evaluated using Eq. (21)) is presented. Grey lines represent estimates using the full Fisher Information matrix (Gauss–Newton method) while black lines represent estimates made using only the diagonal elements of the Fisher Information matrix.

The relative plausibility of the two model structures was measured using a Bayes Factor (computed using Eq. (26)):

$$\beta_{1,2} = \frac{P(\mathcal{D}|\mathcal{M}_1)}{P(\mathcal{D}|\mathcal{M}_2)} \quad (28)$$

such that a high value of $\beta_{1,2}$ indicates that the nonlinear model is more plausible than the linear model. The ability of the linear model to replicate the training data and a plot of $\ln \beta_{1,2}$ as a function of the number of points in the training data are shown in Fig. 7(a) and (b) respectively. It is clear that the plausibility of the nonlinear model relative to the linear model increases greatly when the ability of the linear model to replicate the training data worsens. Upon studying Fig. 8 it is interesting to note that, if one had used between 500 and 1000 data points, it could have been incorrectly concluded that the linear model was preferable.

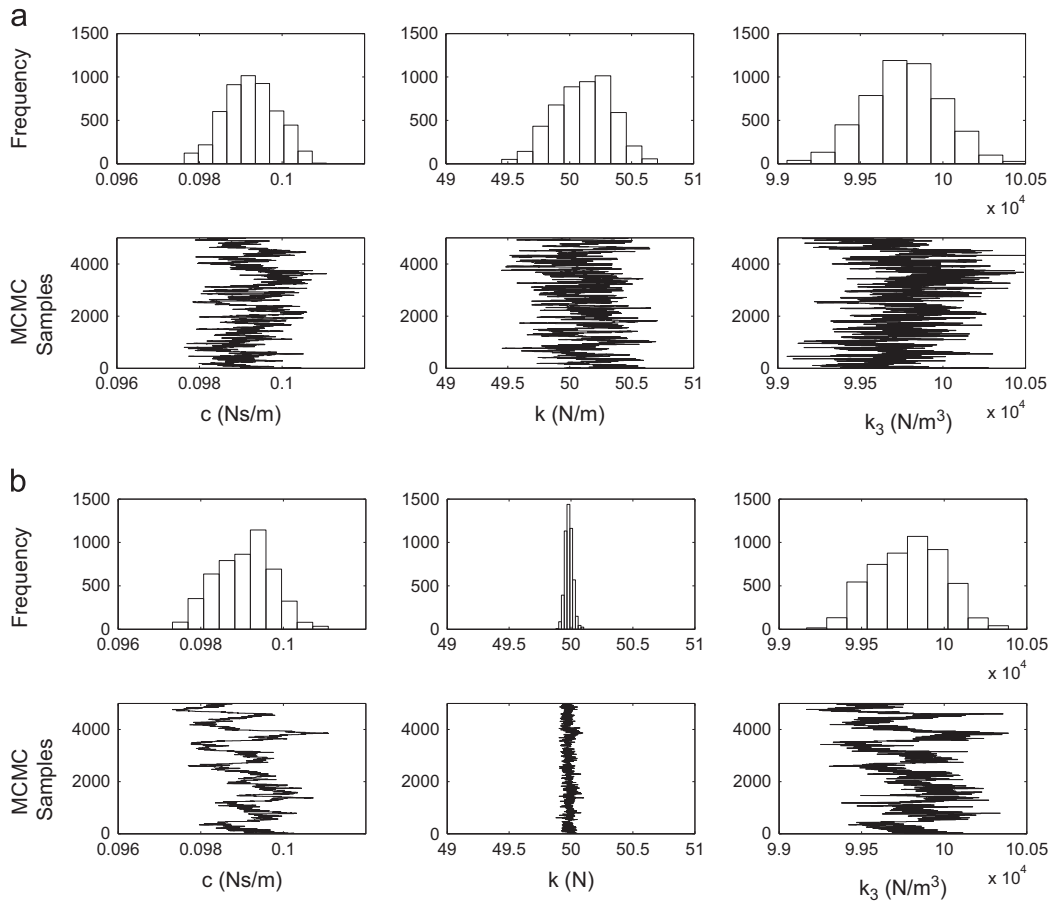


Fig. 6. Parameter estimation of the base excited Duffing oscillator. MCMC samples from the posterior distribution using (a) the first 3500 and (b) the first 4500 points of training data.

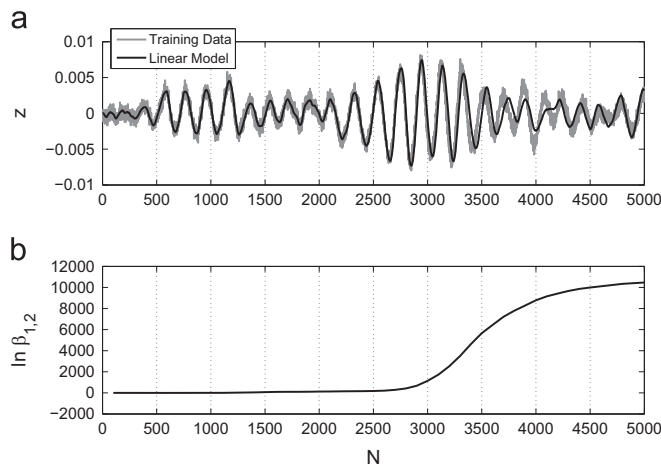


Fig. 7. Selecting a model to replicate the response of the base-excited Duffing oscillator. (a) The ability of the linear model to replicate a set of training data. (b) Bayes Factor as a function of the number of points in the training data (N).

5. Example: system identification of the Tamar Bridge using model emulators

The Tamar Bridge, built in 1961, is situated in South West England. In 2001, in order to meet with EU directives the bridge was strengthened and widened. During this exercise a monitoring system that collects measurements of displacements, cable tensions and environmental conditions was installed in the interest of studying the bridge's performance during the

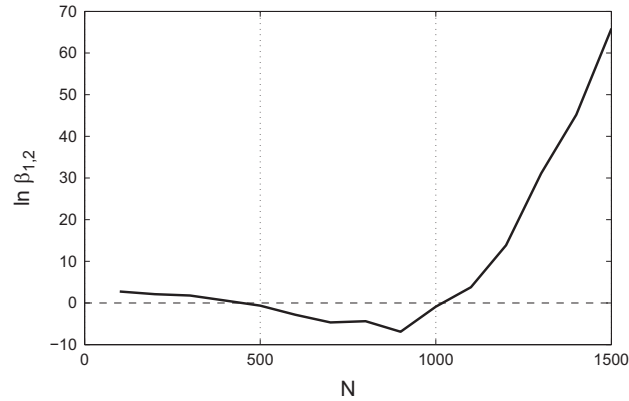


Fig. 8. A close-up view of Fig. 7(b), analysing the variation of Bayes Factor over the first 1500 points of data.

upgrade. Nowadays the monitoring system has been extended to include dynamic measurements, and modal properties extracted from accelerometer measurements using stochastic subspace identification are available.

In order to better understand the dynamic response of the structure to environmental and operational conditions, a number of analyses have been carried out [30]. One such analysis utilised simple response surface models (employing linear regression) to capture the relationship between the extracted deck natural frequency and measured environmental and operational conditions (such as temperature, wind conditions and traffic loading). It was found that simple linear models (that may be thought of here as meta models) were able to account for the majority of the variation in the deck natural frequencies.

The question of model selection and informative training data is of much interest in this case, as a large database (which spans a number of years) is available for learning and contains numerous candidate parameters. The following analysis is concerned with using model emulators to predict the first natural frequency of the bridge specifically.

5.1. Parameter estimation

To begin the analysis it was hypothesised that the first natural frequency of the bridge (denoted ω) could be predicted using a model of the form:

$$\hat{\omega}_n = \theta T_n \quad (29)$$

where T represents the traffic load and θ is a parameter whose most probable value can be calculated through linear regression. In this case an improper prior and, as before, a Gaussian prediction-error model were utilised. Consequently, the likelihood is given by:

$$P(\mathcal{D}|\theta, \mathcal{M}) = (2\pi\sigma^2)^{-N/2} \exp\left(-\frac{1}{2\sigma^2} \sum_{n=1}^N (\omega_n - \theta T_n)^2\right). \quad (30)$$

Differentiating the negative logarithm of Eq. (30) twice with respect to θ allows one to realise an exact expression for A :

$$A = \frac{\sum_{n=1}^N (T_n^2)}{\sigma^2} \quad (31)$$

and, as a result, an exact expression for the Shannon entropy of the posterior:

$$S_\theta = \ln\left(\frac{\sigma^2}{\sum_{n=1}^N (T_n)^2}\right). \quad (32)$$

Interestingly, Eq. (32) implies that one can obtain more information about θ if the training data features large values of T . To explain this one must recall that, through the choice of likelihood, it was assumed that each measurement was corrupted by the same level of noise. As a result Eq. (32) is essentially indicating that *informative measurements are those which are far from the noise floor of the measurement process*. As was pointed out in [24], this demonstrates a flaw in the definition of the likelihood as it assumes that the model will perform equally well over all regions of the input space. That being said, Fig. 9 shows that, in this case, Eq. (32) can be used to accurately determine which parts of the training data are the most informative with regard to the most probable estimate of θ . Fig. 10 shows that there is a reasonably good match between the measured and modelled first natural frequency of the bridge.

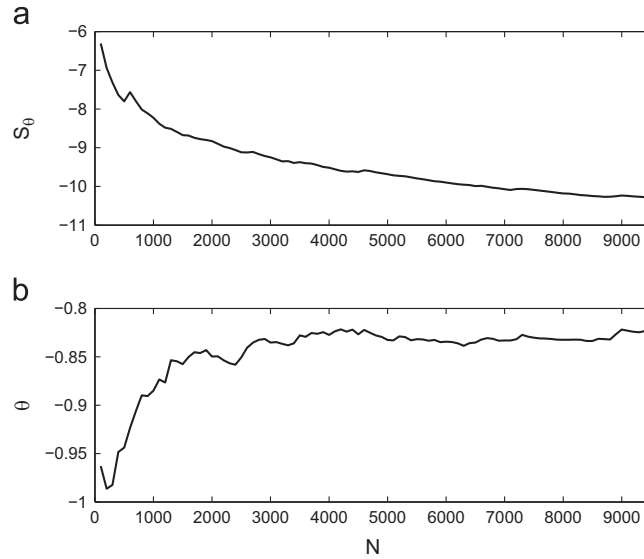


Fig. 9. (a) Shannon entropy of the posterior and (b) most probable parameter estimate for a traffic-dependent model of the first natural frequency of the Tamar bridge.

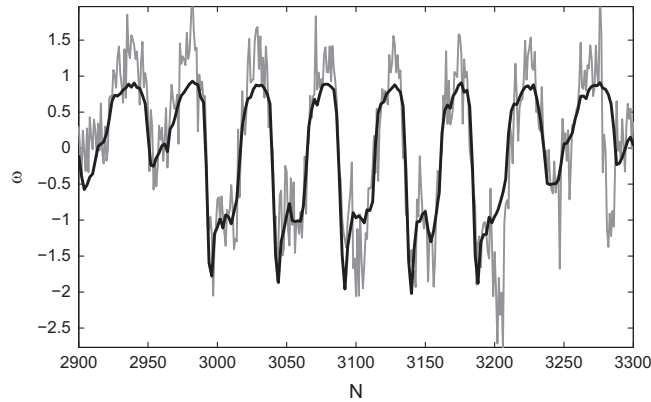


Fig. 10. The measured first natural frequency of the Tamar bridge (grey) compared with that predicted by the traffic-dependent model (black).

5.2. Model selection

In the final example, the issue of model emulator selection is investigated. A set of three candidate model structures are considered, the first is the ‘traffic-only’ model described in the previous section

$$\hat{\omega}_n = \theta_1 T_n. \tag{33}$$

The second model structure is:

$$\hat{\omega}_n = \theta_1 T_n + \theta_2 W_n \tag{34}$$

where W represents wind speed, while the final model structure is:

$$\hat{\omega}_n = \theta_1 T_n + \theta_2 W_n + \theta_3 \tau_n \tag{35}$$

where τ represents temperature. Using the same training data as in the previous section, linear regression techniques were used to identify the most probable parameters of each model. These values and the mean square error (MSE) between the model and the training data are shown in Table 2. It can be seen that the reduction in MSE achieved using model 3 over model 2 seems relatively small compared to the reduction in MSE achieved using model 2 over model 1.

As in Section 4.2, the logarithm of the Bayes Factor was plotted as a function of the number of points in the training data. In this case the relatively simple structure of the models allowed the full Fisher Information matrix to be calculated analytically in a straightforward manner.

Fig. 11(a) shows the relative plausibility of model structure 2 relative to model structure 1. It is clear that using wind as an additional input has made model 2 more plausible than model 1, and that this result becomes more pronounced as

Table 2
Most probable parameters and mean square error for 3 models of the first natural frequency of the Tamar bridge.

Model structure	$\theta_{MP}^{(1)}$	$\theta_{MP}^{(2)}$	$\theta_{MP}^{(3)}$	MSE
\mathcal{M}_1	-0.8233	-	-	0.3239
\mathcal{M}_2	-0.8013	-0.2322	-	0.2672
\mathcal{M}_3	-0.7945	-0.2226	-0.0319	0.2666

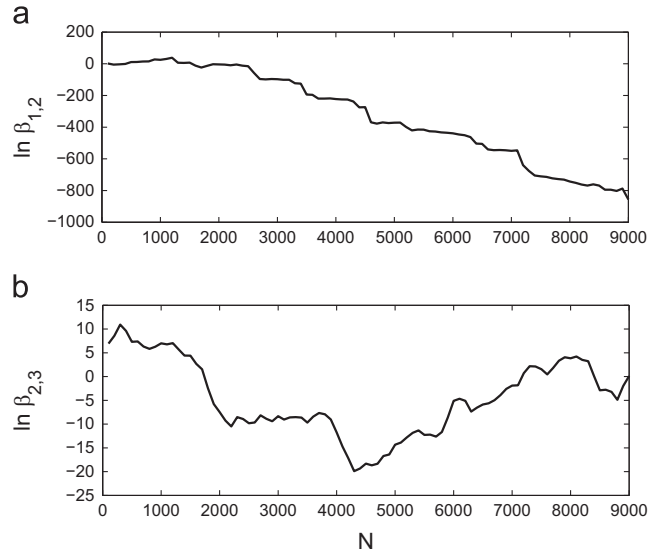


Fig. 11. The logarithms of Bayes Factor for (a) model structure 2 relative to model structure 1 and (b) model structure 2 relative to model structure 3.

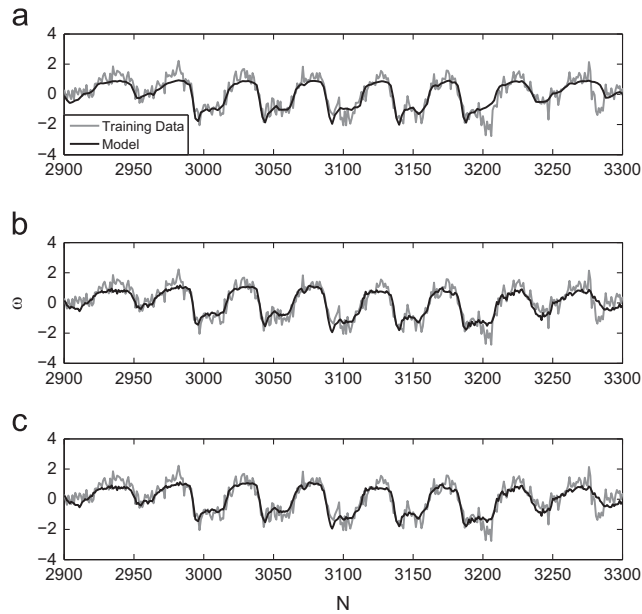


Fig. 12. The ability of (a) model 1, (b) model 2 and (c) model 3 to replicate the measured first natural frequency of the Tamar bridge.

additional training data is used. However, upon studying Fig. 11(b), it is much less clear which out of models 2 and 3 are the more plausible. The key point here is that the relative plausibility of the two models does not become more pronounced as additional data is used. It would be incorrect to interpret this as meaning that model 2 is preferable to model 3. In fact it shows that *this particular set of data does not contain enough information to help us to choose between models 2 and 3*. Recalling that model 3 involves a temperature input it would be interesting to see if a relatively long set of training

data – which included seasonal variations – would be more informative with regard to choosing between these two model structures. This is left as a topic of future work.

For the sake of completeness, the ability of the 3 models to replicate the first natural frequency of the bridge is shown in Fig. 12.

6. Discussion and future work

With regard to model selection, it is assumed throughout this paper that one of the candidate model structures will be much more probable than the others and that, once identified, all future predictions will be made using this model. However, using a full Bayesian approach, one would make future predictions using every model in the set of candidates weighted by their posterior probabilities. This approach is discussed at length in [1] where it is described as ‘hyper-robust predictions using model averaging’. The ability to improve one’s ‘hyper-robust’ predictions using highly informative training data is certainly an interesting topic for future work. It may also be beneficial to see if the concepts detailed in this paper can be applied within the context of Bayesian structural health monitoring [31], in the Bayesian model selection of prediction error models [23] and the recently developed ‘fast Bayesian FFT method’ [32].

In Section 4 the effect of the training data on one’s confidence in individual parameter estimates was shown (Figs. 3 and 4). This analysis was conducted using Eq. (22) – which is based on the assumption that one’s parameter correlations are negligible. It is important to note that this will not always be true and that, in the general case, one should instead calculate the Shannon entropy using Eq. (21) (as shown in Fig. 5).

Finally, it is again emphasised that the work presented here addresses the situation where one is *presented* with a large set of training data – this is different from situations where one can easily generate more data using additional experimental tests. The latter situation was investigated by Metallidis et al. [26] where, with the aim of detecting faults in vehicle suspension systems by monitoring parameter estimates, the Shannon entropy was used to identify the experimental conditions which would lead to the greatest reduction in parameter uncertainty. It is interesting to note that, in [26], the optimum experiment was defined as that which revealed the most information about one’s parameter estimates while, in the current paper, it is suggested that training data also needs to provide information with regard to model selection. A potentially useful avenue of future work could involve combining these ideas – the goal being to design experiments which are informative with regard to both model selection and parameter estimation.

7. Conclusions

This paper was concerned with the scenario where, with the aim of performing Bayesian system identification, one is presented with extremely large sets of training data. It addresses the situation where, through using a subset of the available data, one is able to make significant computational savings when running MCMC – something which is particularly important if one is constrained to using relatively expensive physics-based models. To that end, within the context of a Bayesian framework, an analytical expression approximating the effect of sets of training data on the posterior parameter covariance matrix was derived. This was then linked to previous work from the machine learning community in which the ‘informativeness’ of training data was measured using the Shannon entropy of the posterior parameter distribution. With regard to the system identification of dynamical systems, it was then shown that the concepts developed in this paper can be used to select subsets of data which – with regard to both parameter estimation and model selection – are highly informative. Examples include the system identification of a base-excited Duffing oscillator using physics-based models and of model emulators which were used to predict the first natural frequency of the Tamar bridge.

Acknowledgments

This paper was funded by an EPSRC fellowship and the EPSRC Programme Grant ‘Engineering Nonlinearity’ EP/K003836/1.

References

- [1] J.L. Beck, Bayesian system identification based on probability logic, *Struct. Control Health Monit.* 17 (7) (2010) 825–847.
- [2] D.J.C. MacKay, Bayesian interpolation, *Neural Comput.* 4 (3) (1992) 415–447.
- [3] J.L. Beck, L.S. Katafygiotis, Updating models and their uncertainties. I: Bayesian statistical framework, *J. Eng. Mech.* 124 (4) (1998) 455–461.
- [4] J.S. Liu, Monte Carlo strategies in scientific computing, in: Springer Series in Statistics, Springer, New York, USA, 2008.
- [5] R.M. Neal, Probabilistic Inference using Markov Chain Monte Carlo Methods, Technical Report, University of Toronto, 1993.
- [6] D.J.C. MacKay, Information Theory, Inference and Learning Algorithms, Cambridge University Press, New York, USA, 2003.
- [7] S. Kirkpatrick, C.D. Gelatt Jr., M.P. Vecchi, Optimization by simulated annealing, *Science* 220 (4598) (1983) 671–680.
- [8] H. Szu, R. Hartley, Fast simulated annealing, *Phys. Lett. A* 122 (3–4) (1987) 157–162.
- [9] L. Ingber, Very fast simulated re-annealing, *Math. Comput. Model.* 12 (8) (1989) 967–973.
- [10] P. Salamon, J.D. Nulton, J.R. Harland, J. Pedersen, G. Ruppeiner, L. Liao, Simulated annealing with constant thermodynamic speed, *Comput. Phys. Commun.* 49 (3) (1988) 423–428.
- [11] J.L. Beck, S.-K. Au, Bayesian updating of structural models and reliability using Markov Chain Monte Carlo simulation, *J. Eng. Mech.* 128 (4) (2002) 380–391.

- [12] J. Ching, Y.C. Chen, Transitional Markov Chain Monte Carlo Method for Bayesian model updating, model class selection, and model averaging, *J. Eng. Mech.* 133 (7) (2007) 816–832.
- [13] J.L. Beck, K.M. Zuev, Asymptotically independent Markov sampling: a new Markov Chain Monte Carlo scheme for Bayesian inference, *Int. J. Uncertain. Quantif.* 3 (5) (2013).
- [14] K. Worden, J.J. Hensman, Parameter estimation and model selection for a class of hysteretic systems using Bayesian inference, *Mech. Sys. Signal Process.* 32 (2012) 153–169.
- [15] P.L. Green, K. Worden, Modelling friction in a nonlinear dynamic system via Bayesian inference, *Top. Modal Anal. II* 6 (2012) 657–667.
- [16] S. Duane, A.D. Kennedy, B.J. Pendleton, D. Roweth, Hybrid Monte Carlo, *Phys. Lett. B* 195 (2) (1987) 216–222.
- [17] S.H. Cheung, J.L. Beck, Bayesian model updating using hybrid Monte Carlo simulation with application to structural dynamic models with many uncertain parameters, *J. Eng. Mech.* 135 (4) (2009) 243–255.
- [18] Becker, K. Worden, J. Rowson, Bayesian sensitivity analysis of bifurcating nonlinear models, *Mech. Sys. Sig. Process.* 34(1), 57–75.
- [19] P. Angelikopoulos, C. Papadimitriou, P. Koumoutsakos, Bayesian uncertainty quantification and propagation in molecular dynamics simulations: a high performance computing framework, *J. Chem. Phys.* 137 (14) (2012) 144103.
- [20] H. Akaike, A new look at the statistical model identification, *IEEE Trans. Autom. Control* 19 (6) (1974) 716–723.
- [21] G. Schwarz, Estimating the dimension of a model, *Ann. Stat.* 6 (2) (1978) 461–464.
- [22] J.L. Beck, K.V. Yuen, Model selection using response measurements: Bayesian probabilistic approach, *J. Eng. Mech.* 130 (2) (2004) 192–203.
- [23] E. Simoen, C. Papadimitriou, G. Lombaert, On prediction error correlation in Bayesian model updating, *J. Sound Vibration*, 332(18), 4136–4152.
- [24] D.J.C. MacKay, Information-based objective functions for active data selection, *Neural Comput.* 4 (4) (1992) 590–604.
- [25] C. Papadimitriou, J.L. Beck, S. Kui Au, Entropy-based optimal sensor location for structural model updating, *J. Vib. Control* 6 (5) (2000) 781–800.
- [26] P. Metallidis, G. Verros, S. Natsiavas, C. Papadimitriou, Fault detection and optimal sensor location in vehicle suspensions, *J. Vib. Control* 9 (3–4) (2003) 337–359.
- [27] C. Papadimitriou, Optimal sensor placement methodology for parametric identification of structural systems, *J. Sound Vib.* 278 (4) (2004) 923–947.
- [28] E.T. Jaynes, G.L. Bretthorst, *Probability Theory: The Logic of Science*, Cambridge University Press, New York, USA, 2003.
- [29] Y. Bard, *Nonlinear Parameter Estimation*, Academic Press, New York, USA, 1974.
- [30] E.J. Cross, K.Y. Koo, J.M.W. Brownjohn, K. Worden, Long-term monitoring and data analysis of the Tamar Bridge, *Mech. Sys. Sig. Process.* 35(1), 16–34.
- [31] M.W. Vanik, J.L. Beck, S.K. Au, Bayesian probabilistic approach to structural health monitoring, *J. Eng. Mech.* 126 (7) (2000) 738–745.
- [32] S.K. Au, Fast Bayesian FFT Method for ambient modal identification with separated modes, *J. Eng. Mech.* 137 (3) (2011) 214–226.